Experimental Tests to Validate the Simulation Model of a Domestic Trigeneration Scheme with Hybrid RESs and Desalting Techniques

J. Uche*
CIRCE Research Institute.
Department of Mechanical Engineering. University of Zaragoza
email: javiuche@unizar.es

A. Muzás
Department of Mechanical Engineering
University of Zaragoza
email: andresmuzas8@gmail.com

L.E. Acevedo
Area of Energy and Environmental Technologies
CIRCE Foundation
email: lacevedo@fcirce.es

S. Usón
CIRCE Research Institute.
Department of Mechanical Engineering. University of Zaragoza
email: suson@unizar.es

A. Martínez
CIRCE Research Institute.
Department of Mechanical Engineering. University of Zaragoza
email: amayamg@unizar.es

A.A. Bayod
CIRCE Research Institute.
Department of Electrical Engineering. University of Zaragoza
email: aabayod@unizar.es

ABSTRACT

Experimental tests of a small polygeneration plant unit based on hybrid renewable energy and desalination have been used to validate a novel model simulation of this plant. It provides electricity by coupling photovoltaic/thermal collectors and a micro-wind turbine, fresh water by means of hybrid desalination (membrane distillation, and reverse osmosis), and sanitary hot water coming from the photovoltaic/thermal collectors and an evacuated tubes collector. Plant was designed to operate in off-grid conditions and conventional energy storage systems were used (lead acid batteries and hot water tank). Simulation model was performed in TRNSYS environment and it was fully validated by comparing several key plant measurements. The analysis was focused on five typical days of summer, fall and winter. Some differences found in experimental and simulated values were analysed. To reduce those gaps, some modifications have been suggested to the model or the pilot unit respectively. As a result, a validated model in TRNSYS of the plant was obtained. This model can be used for the further scale up of new projects to cover any other scheduled demands of power and water in isolated areas, whenever is based on the combination of the abovementioned technologies.

* Corresponding author

KEYWORDS

Desalination, renewable sources, trigeneration, hybrid systems, simulation, experimental validation.

1. Introduction

Safe and sustainable provision of power and water is an emerging issue, which can be stressed in case of not having power and water networks. In other words, the water-energy-nexus (WEN) for isolated communities requires a systemic approach [1]. Integrated renewable energy sources (RES) are now a widely extended sustainable solution that can be easily adapted to cover specific or local demands [2], and the planning of a sustainable solution for isolated islands has been extensively studied [3]. Hybrid RES are commonly utilized in isolated areas since electricity one energy device can offset the shortfall of the other and then the load demands are better matched [4]. Integrated schemes considering energy storage in isolated areas [5-6] or local communities [7] has also been taken into account, being water the energy storage media. Hybrid devices like the photovoltaic-thermal collectors (PVT) can also provide power and heat simultaneously as a green cogeneration [8]. On the other hand, the use of RES in desalination has also been extensively analysed due to its energy intensity for the whole portfolio of existing techniques. Reverse Osmosis (RO) is maybe the most experienced technology [9] due to its low energy consumption and modularity, but solar thermal energy can also easily couple with distillation methods to provide water [10]. Water from moist air can also be extracted to produce some amount of water coming from RES [11-12]. New developments related to direct solar desalination by recent materials, or improved Membrane Distillation (MD) by using photothermal materials show that solar desalination is an emerging issue [13]. Anyway, storage required is a crucial constraint to maintain a reliable operation in desalting processes [14]. To provide a continuous and safe supply to desalination facilities, hybrid RESs schemes have been usually combined. A well-known set is linking photovoltaics and wind energy [15], but some different solar devices can also be hybridized to distillate seawater [16]. Alternatively, hybrid desalination has been also promoted in order to provide a constant supply of fresh water [17-18], and solar power has been proposed to supply thermal and membrane desalination [19] or dual solar distillers [20]. In any case, the combination PV+Wind linked to RO seems to be the technological trend [21], and extensive literature can be found related to its optimization, being new generation of artificial intelligence algorithms a good candidate to substitute conventional optimization methods [22].

In this context, the use of RES to supply polygeneration schemes and not only desalination is playing an increasing role. They could constitute a sustainable solution for the aggregated amount of demands in the small isolated communities. In this sense, Calise and co-workers have been analysed in depth several integrated configurations of polygeneration schemes based on RES including power, heating and/or cooling and desalination [23-29]. Solar and sometimes geothermal are the renewable sources used to design the polygeneration schemes. Other researchers have also analysed the performance of polygeneration schemes producing power and desalted water with solar fields [30-32], heating, cooling and water [33] or power, heating and distilled water [34]. Geothermal was also tested to provide power, hot sanitary water and fresh water [35]. Concentrated solar power has also been promoted to provide power, heat, cooling and water [36-37]. When hybrid RES are combined to polygeneration, the state of the art is reduced to a rather small number of examples, being only found some optimization schedules based on PV and wind to supply water and power [38], diverse solar fields to produce hydrogen and water [39], or solar and biomass to produce power, cooling

and distillate water [40]. To sum up, the state of the art reveals that very few experimental tests on trigeneration or polygeneration schemes involving seawater desalination and RES can be found in literature. If the hybrid production of electricity and water can be complemented, the offer is practically inexistent. Nevertheless, if the three demands of power (W), fresh water (FW) and sanitary how water (SHW) can be supplied by two complementary techniques, robustness and flexibility makes that plant a definite solution in isolated areas. This double combination of hybrid techniques based on RESs (to provide electricity and heat), desalination (to supply fresh water) and SHW by consuming power or heat was previously tested by the authors. More details about the test campaign can be found in [41].

Previous state of the art also reflects that most of the integrated analysis of energy and water production is based on different simulation tools. Specific software required by a subsystem in the scheme could be used for the photovoltaics (PV) and Reverse Osmosis (RO) coupling [16] or a hybrid solar cogeneration of power and water [42]. A unique software to analyse the whole polygeneration scheme like Matlab [43], Aspen [44] or EES [45] were also the chosen alternatives, and sometimes there is not an explicit mention to the used software [40] or is a combination of integrated packages [46]. In any case, TRNSYS is the most widely used software to deal with proposals of polygeneration schemes including RES and desalted water. Calise and colleagues always used that software in their analyses [23-29], but some other researchers have also used this tool to analyse the performance of polygeneration schemes based on solar energy [33] or to optimize the first design [47].

However, it is not so easy to find out a long list of experimental facilities to both provide power and water. For instance, in [48] Raluy et al. tested the direct coupling of flat plate collectors (FPC) helped by a PV system linked to membrane distillation (MD). A similar configuration for a higher MD production was found in [49], or a modified PVT coupled to a solar still [50]. One practical example in the abovementioned state of the art can be found in [15] for hybrid RES and in [20] for solar hybrid desalination. Solar thermal polygeneration presented by Mohan et al. in [33] was also tested in the UAE environment [51].

On the other hand, the comparison between simulations and experimental tests is quite usual in order to validate that simulation for further analyses, or to improve the plant performance in the sense of finding some bottlenecks from measurements that by far are not expected by the model predictions. For instance, in solar distillation some tests of a Direct Contact MD supplied by solar energy modelled in Matlab [52], Aspen [53] or DVODE [54] were compared with. Hybrid RESs generation has also been validated in this way [55,56]. Of course, TRNSYS is again the most widely used software to validate experimental test or to complement future studies: from the study of the PV+RO system [57], solar systems based on PV or PVT [58-61] or trigeneration units for the residential sector [62-63]. Sometimes, validation of this simulation is carried out by other integrated experimental facilities that generated power and water [30,40], alternative fuels [64], or even comparing with simulations performed by other authors [39]. Again, the experimental validation of a model based on hybrid combinations for power and water are not found in literature.

To sum up, in this paper, representative experimental tests of the innovative pilot unit presented at [41] have been used to validate a new simulation model of the plant developed in TRNSYS17. Preliminary design of the hybrid trigeneration unit was performed in TRNSYS16 including a sensitivity analysis of some design parameters and the economic liability of the pilot unit [65]. Definite design was later extended to study the performance, technical improvements on the grid and economic profit in case of having a similar but on-

grid pilot unit [66]. Exergy and exergy cost analysis have also been implemented to identify and then to reduce local irreversibilities in the hybrid pilot unit [67]. As the model has been introduced by the experimental test managers, detailed controls embedded in the pilot unit were as far as possible introduced in the model, in order to fairly check if simulation and the pilot unit have a similar behaviour. Furthermore, validation has been extensively made on the whole set of measures collected in the control system of the pilot unit. Very close values in simulation and tests were finally found for the daytime selected tests after the fine-tuning of the model. Consequently, model validation could be assumed for this configuration type. Accordingly, with this model the door could be open to the scale-up of new designs of this innovative scheme based on hybrid RES and desalination. They can be easily mounted for any other demands of power, water and SHW in isolated areas at affordable costs.

2. Materials and methods

The structure of the paper is as follows. In this section, first, the pilot unit is physically described, and the main technical characteristics are also given. Second, TRNSYS model developed to validate the pilot unit is detailed. Third, selected daytime tests and parameters to validate the unit and the model are presented. Section 3 includes the comparative analysis of the selected tests, in terms of statistical parameters as well as found deviations confronting the unit and the model. Finally, in section 4 main conclusions and the applicability of the validated model are exposed.

2.1 Plant description

The experimental facility (see Figure 1) was installed on the roof and the attic of an industrial unit located in the northern Campus of the University of Zaragoza (Latitude 41.6865 North, Longitude -0.8878 West). The solar loop is composed of five solar collectors (four PVT collectors, 240 W_p, 1.63 m^2 each and one Evacuated Tube Collector –ETC– of 3 m^2), a solar pump and the hot water tank (HWT, 325 L). Solar collectors have a tilt of 40º and are totally south-oriented. Heated water-glycol solution is driven by a pump working upon a hysteresis control loop if the ETC outlet temperature is in the range 7-2°C above the mean HWT temperature. The MD unit (20 L/h max.) is fed by the HWT through a heater (HX-MD). Alternatively, the HWT could serve the SHW demand. Those flows delivered to MD (Q_{HX-MD}) or SHW (Q_{SHW}) are controlled by a proportional commanded valve. MD is usually activated at 70°C, although lower temperatures could start the unit with less distillate rates. The MD pilot unit is a commercial Permeate Gap type (PG) module and consists of a spiral wound desalination membrane with an effective area of 10 m^2. The SHW discharge from the HWT is usually blended with tap water to serve at the service temperature (45°C). To avoid overheating in the solar loop, an air-cooled heat exchanger (HX-AC) and the self-emptying of the HWT were implemented in the control system.

Regarding the power loop, the four PVTs and batteries were connected by a maximum power point tracker (MPPT) device and a charge controller. A 400 W_p micro-wind turbine (WT) was also connected in parallel with the two lead acid batteries in series (250 Ah, 12 V). Most of that power can be converted into AC by means of a regulator/inverter (1 kW). Internal consumption comes from solar pump (P_{SL}, 50 W), seawater pump to feed the MD unit (P_{MD}, 80 W), hot water pump that feeds the MD (P_{HX-MD}, 60 W) and the HX-AC fan (30 W). Domestic internal power demand is regulated by an AC potentiometer connected to an electric resistance (ER) of up to 1 kW. Finally, the RO unit consumes DC power from the batteries and permeates up to 30 L/h with a constant power consumption of about of 100 W. A minimum SOC of 40% is required to maintain the safe operation to the RO pump (> 22 V) in daytime tests. Seawater (SW) tank

(SWT, 450 L) feeds both the RO and MD units and collects their brines. This constitutes a typical solution adopted in this kind of pilot desalination units. The MD unit includes for research purposes a cooling circuit (a new water-cooled HX consuming tap water, HX-CW) to avoid overheating in the SWT, since brine returns to the SWT from the MD evaporator (hot canal) at warmer temperatures (around 7°C higher) and that brine corresponds to about the 98% of the seawater feed flow. On the contrary, RO recovery rate is about the 10% (that is, RO pump delivers 300 L/h) and brine and permeate are not heated during the desalting process.

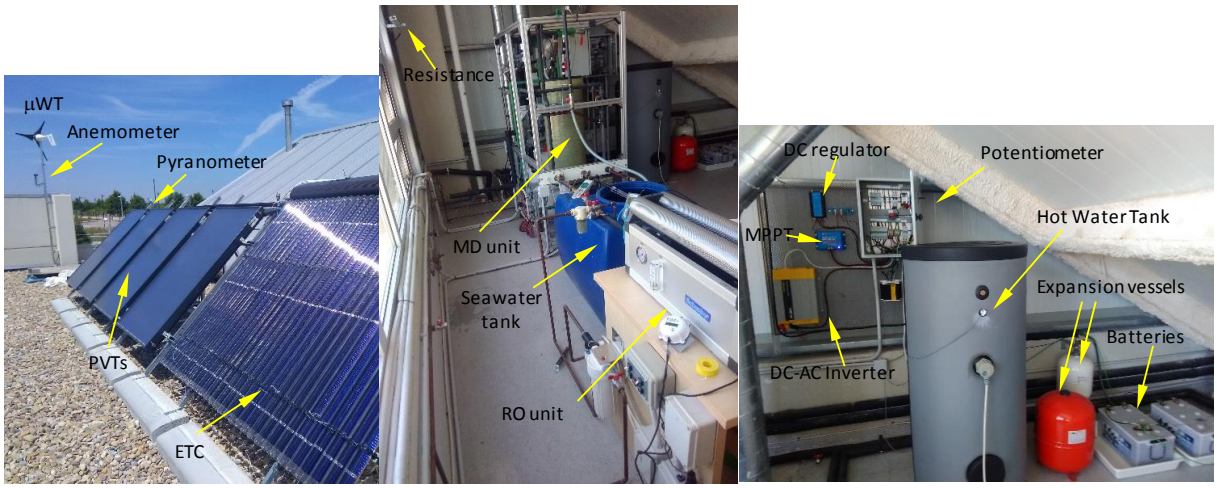

Figure 1. RES devices (left), water providers (center) and energy storage (right) pilot plant subsystems

Control and monitoring system was gradually completed according to development of tests. Fifteen PT-100 sensors were installed. A pyranometer, an anemometer, and a battery controller were also installed in the pilot unit. Measurements were recorded every minute. Plant operation is not fully automatic, since six visual flow meters and three conductivity meters had to be installed. Furthermore, MD operation was characterized by a rather unsteady behaviour. A safe and flexible plant operation according to some established constraints was also implemented by the automata. For instance, SHW pump starts and the SHW valve opens in case of the HWT temperature exceeds 75°C and therefore HWT reduces its temperature. Besides, fan heater HX-AC boots if ETC outlet temperature is higher than 85°C or the outlet PVT temperature is over 80°C. Figure 2 shows the layout of the plant, including the installed sensors.

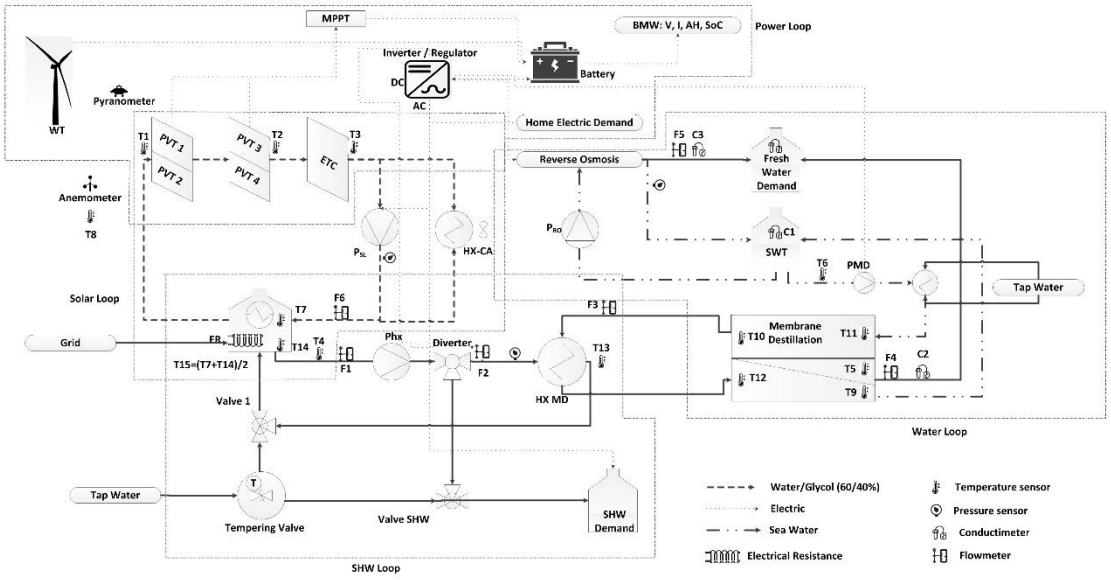

Figure 2. Sketch of the hybrid trigeneration unit.

Table 1 lists the detailed relative uncertainty U(%) of the measured variables in this plant according to the installation previously depicted in Fig. 2. A more detailed description of the pilot plant can be found in [38].

Table 1. Relative uncertainty (U, %) of the pilot plant measurements

Measurement	Point / Instrument	U (%)
Flow rate (F)	SHW to MD/SHW demand	3.2
	SHW to MD	3.2
	SW to MD	6.0
	RO permeate	6.5
	MD distillate	6.9
	Solar loop	9.7
Conductivity (C)	Seawater	0.5
	RO permeate	2.0
	MD distillate	2.0
Current (I)	Battery	0.4
Voltage (V)		0.3
State of Charge (SOC)		0.2
Temperatures (T, 15)	PT-100 class AA	0.2-0.27
Irradiation	Pyranometer	2.6
Wind speed	Anemometer	2.1

Experimental tests on plant devices were individually carried out in the period from November 2016 to May 2017 in this order: PVT, WT, lead-acid batteries, RO and MD. A specific campaign was made on the later by using both the electric resistance of the HWT and solar energy to study its performance in steady and unsteady conditions [68]. Tests on trigeneration mode started in May 2017. Here the three demands were produced according to weather conditions and energy storage levels in the plant. Then, from June 2017 to March 2018 the pilot unit operated to serve

scheduled hourly power, water and SHW demands. A total of 64 tests with an average time of approximately 6 hours were carried out. Detailed estimation of the hourly demands of power, fresh water and SHW was based on the typical consumption patterns of a single family home in Spain [69-70] and existing Spanish regulation [71] for on-grid domestic installations. It was assumed that a 1000 L fresh water tank was previously installed in the single family home. Thus the RO and/or MD operation were oriented to cover daily requirements during the daytime and accordingly, hourly demands of fresh water were usually exceeded by far in performed tests. Complete reported results were included in [41], but summarizing briefly it can be said that high coverage rates were found in most of them except from the period from November to January. Apart from some rainy periods, main limitation of this period was provoked by the very limited incoming radiation due to the partial shading of the adjacent industrial unit.

2.2 TRNSYS model

A detailed new model has been implemented in TRNSYS17 to simulate the plant response according to the scheduled power and water demands. Available types have been used in most of the cases. Fine tuning of the type coefficients was initially made by contrasting the individual tests of the plant devices. Figure 3 shows the main sketch of the TRNSYS model implemented to validate the hybrid RES-based pilot unit, and table 2 presents the types selected to model the plant.

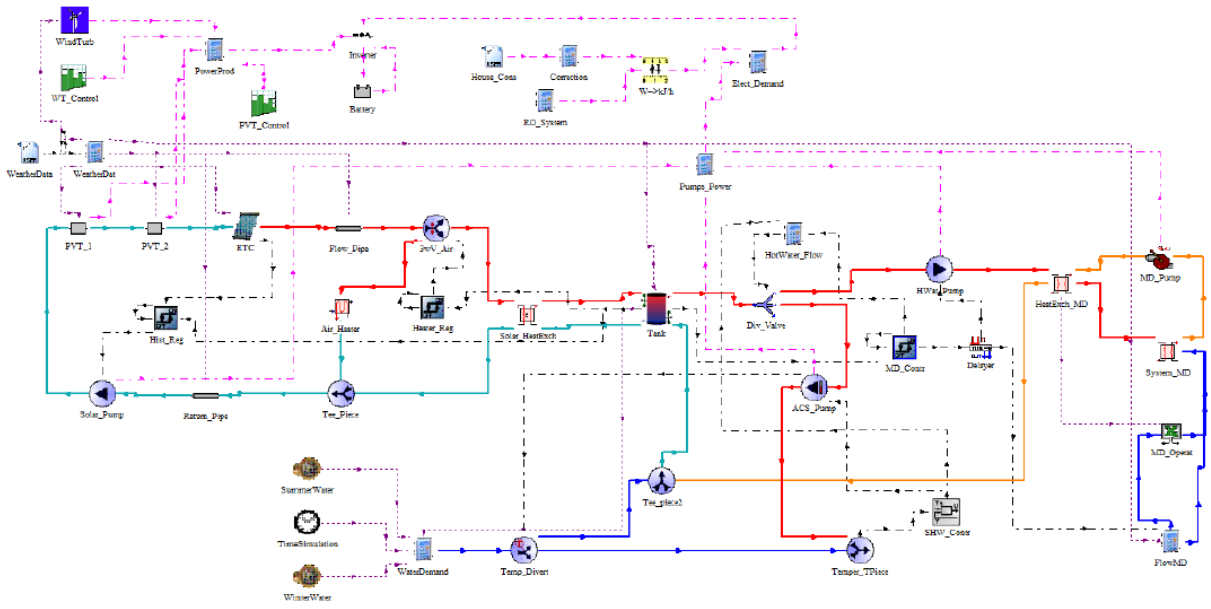

Figure 3. TRNSYS17 layout of the hybrid trigeneration unit.

Table 2. List of TRNSYS types used

Area	Device	Type Number
Solar loop	PVT panel	50
	ETC panel	71
	Pipes	31
	3 ways-valve	11f
	HX in HWT	91
	Solar pump	114
	Air cooler	5g

	Pump controller	2b
	AC controller	2b
SHW loop	Tank (stratified)	4c
	T-pieces	11h
	Diverting valve	647
	SHW pump	110
	SHW controller	22
	SHW demand	14b
MD system	MD pump	742
	HX (to MD)	5b
	Delayer	661
	HX (in the MD)	5b
	D produced	62 (ANN)
	MD controller	2-AquastatC
Power system	WT	90
	WT control	14h
	PVT control	14h
	Inverter	48c
	Battery	47b
Inputs/outputs	Weather data	9a
	FW and SHW demands	9a
	House_ Cons	9a
	Online plotters	65b

In order to validate any test, text file (*WeatherData*, see Figure 2) including one-minute measured wind velocity and irradiation was introduced to further estimate power and heat generated by the WT, PVT and ETC respectively. Regarding demands, now the text file *House_Cons* provided the house power demand per minute requested in the test, following the Spanish consumption patterns. SHW demand was provided by the function editor tool (*WinterWater* and *SummerWater*), giving a different profile along the day in those two periods. Fresh water was then estimated by assuming that the 35% of that fresh water was heated for domestic purposes.

Details of the solar loop are included as follows. In PVT types (*PVT_1* and *PVT_2* in Figure 2), optical efficiencies of 0.69 and loss coefficients of 2.59 $W/m^2 \cdot K$ and 0.058 $W/m^2 \cdot K^2$ were taken. In case of the *ETC*, optical efficiency was reduced up to 0.51, being the loss coefficients 0.92 $W/m^2 \cdot K$ and 0.001 $W/m^2 \cdot K^2$ respectively. Solar loop circulated 100 L/h with a 60/40 water-glycol mixture. Specific heat of that fluid was 3.7 kJ/kg·K. Pipes length totalize 20 meters, with a loss coefficient of 0.05 $W/m^2 \cdot K$ and a diameter of 2 cm. A HX connects the solar loop with the HWT (*Solar_HeatExch*). Note that all HXs in the plant were adapted to validation with an effectiveness in the range 80-90%. HWT is composed by 4 nodes, and thermal losses accounted for 2.5 $KJ/h \cdot m^2.ºC$. A similar control loop (7/2ºC) was maintained in the regulator, being the air cooler (*Air_Heater*) activated at the same set point that in the experiments (85ºC).

Regarding the power loop, WT model (*WindTurb*) selected is WECS Enercon E40 600/46, having the nominal power of 400 W at 12 m/s and the starting velocity at 4 m/s (25 W). Site shear exponent selected was 0.14, the one corresponding to short grasses. *WT_control* and *PVT_control* are two controllable pulse profiles to analyse WT and PVT independently, if desired. The FV efficiency in the PVT type was 14.6% with a temperature loss coefficient of

0.25%/ºC. Batteries type were modelled in mode 2, the one corresponding to Shepherd equations, power given as input (*Battery*). The cell energy capacity is 250 A·h, with 12 cells in series (1 cell in parallel); the charging efficiency is 0.9, and the maximum values per cell charging for current and voltage are 20.5 A and 2.5 V respectively. Finally, as RO consumption is fixed (3.6 kW/m^3), this power demand was introduced in *RO_System* if the RO unit was put into operation.

The SHW loop contains several junctions and diverters in order to serve SHW to the demand at the service temperature (45ºC) or the MD, as well as to fill in the HWT. Anyway, specific models were required for PG-MD model since this device is not included in the types library. In the preliminary model made in TRNSYS16, a simple regression model was used to estimate distillate produced as a function of the seawater input flow (with a heat capacity of 3.95 kJ/kg·K) and the temperatures of the seawater entering the hot and cold MD canals. However, in the new version test data obtained served to create an artificial neural network (ANN) to predict the PG-MD distillate as a function of the same three inlet parameters [68]. In this manner, distillate produced in the ANN is independent from the heat source type (thermal or electrical). TRNSYS calculated distillate by calling the Excel sheet (*MD_Operat*) with the ANN coefficients linked to those three inlet constrained parameters. It should be pointed out that out of the trained ranges, the ANN result is not guaranteed (please refer to [68] for more information about the operation limits). Heat transfer combined by the aforementioned mass transfer process in the MD was completed by the inclusion of a new HX, thus the MD unit is fully modelled (*System_MD*). A similar one (*HeatExch_MD*) supplies the heat to the MD unit and returning that heat to the HWT, being the SHW flow pumped (*HotWat_Pump*) to that HX the same that the regulated in the tests. Finally, to consider that MD unit requires, on average, 20 minutes to produce some amount of distillate from its heating, a delay function (*Delayer*) was required to accommodate as much as possible simulated and measured values.

2.3 Model validation

Taking into account that the majority of the tests were not carried out in consecutive days and only were carried out in daytime since the industrial unit is not operative at night-time, model validation has been focused on the analysis of some representative daytime tests. Thus, weather data entering the TRNSYS17 model was adopted to any compared single daytime test. Consequently, global parameters like annual productions or the energy efficiency assessment of the whole plant were not used to validate the model although these figures can be found in [41]. Five days have been selected for the analysis, corresponding to rather long tests and diverse environmental conditions or operating decisions taken on the pilot unit:

- 10/08/2017: A representative sunny (but partly cloudy at the end) and windy daytime. In this test PVT were disconnected to the batteries up to 11:45 approximately. Furthermore, HWT temperature was not able to feed the MD unit up to 14:00.
- 08/09/2017: A representative sunny and gentle wind daytime. At noon the flowrate of seawater to MD was suddenly reduced from 350 to 300 L/h in the provision of not enough thermal energy to maintain its operation.
- 02/10/2017: A sun/cloud mix daytime (mainly the afternoon) with calm winds. This third test is characterized by the full load of the battery at the beginning (SOC=100%).
- 06/03/2018: A sunny and gentle wind daytime in winter period. HWT is rather high from the daytime test of the previous day. Full load of the battery initiated the test.
- 07/03/2018: A sun/cloud mix daytime with breeze. HWT temperature is not enough to activate the MD that daytime test.

Time step of the model and measured data were forced to be the same value (1 minute). Table 3 shows main data of the three days considered, as well as averaged data of the test campaign. Detailed productions of electricity (E_{PU}) from the pilot unit and power demand served to the family (E_H), SHW and desalted water (FW), coverage rate of the predicted demands (CR, %), and specific consumptions found in the two hybrid desalting units (SEC) can be seen in that table. Energy storage variation in the HWT (ΔT) and batteries (SOC) during that daytime tests are also included, as well as the thermal fraction provided by the PVT (TF_{PVT},%) and the power fraction coming from the WT with respect the total power produced (WF_{WT},%).

Table 3. Accumulated productions, demands coverage rate, specific consumptions and energy storage variation in the three selected tests

Date of test	10/08/17	08/09/17	02/10/17	07/03/18	06/03/18	Avg.
Duration (min)	498	581	257	517	339	356
E_{PU} (Wh)	3056.6	3664.9	2202.8	3470.4	1394.5	2103.2
E_H (Wh)	2251.1	2521.8	1087.7	2410.3	1350.3	1552.1
FW_{RO} (L)	212.43	239.58	105.85	212.08	138.50	138.0
FW_{MD} (L)	19.35	54.02	36.00	50.28	0	29.6
FW (L)	231.78	293.60	141.85	262.36	138.50	160.2
SHW (L)	24.41	50.13	38.69	36.95	40.89	68.6
CR_E (%, test)	97.55	100.21	124.14	99.32	96.96	--
CR_{FW} (% day)	81.55	103.17	49.61	86.26	45.71	--
CR_{SHW} (% test)	128.77	115.34	170.12	94.86	203.07	--
SEC_{RO} (kWh/m^3)	3.54	3.68	3.68	3.66	3.67	3.66
SEC_{MD} (kWh/m^3)	296.20	303.73	242.04	262.7	--	293.2
ΔT_{HWT} (°C)	14.10	-13.10	-0.30	-1.15	5.75	--
ΔSOC (%)	-13.40	-15.80	-0.70	-15.20	-2.80	--
TF_{PVT} (%)	75.5	78.9	77.3	78.4	34.2	--
WF_{WT} (%)	3.4	0.4	3.0	0.5	4.9	--

Figure 4 depicts the evolution of the environmental conditions (external temperature EXT, wind velocity v and solar irradiation to panels G). Three productions of the trigeneration unit in the first selected date (10/08/2017) are also presented: power demand (W,DEM), SHW demand (SHW,DEM), permeate from the RO (Fp) and distillate from the MD (Fd). Note that summer time in Spain (2 hours ahead) and not solar time is used in the Figure.

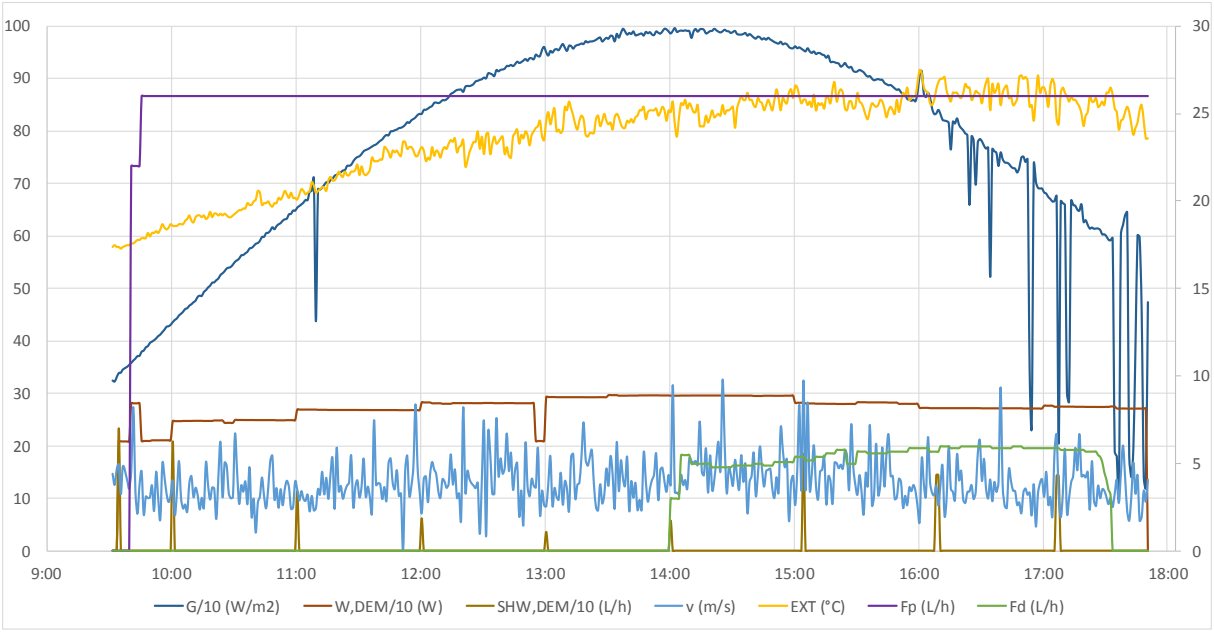

Figure 4. Irradiation and power internal demand (left scale), wind speed, external temperature and water (by the RO and MD) and SHW production (right scale, 10/08/2017).

Measured parameters used for validation are the next:

- Solar loop temperatures (entering and leaving the PVT, iPTV, oPVT, and leaving the ETC, oETC)
- Hot water tank temperatures (upper, lower and medium, uHWT, dHWT, mHWT).
- Temperatures leaving the cold side (condenser, oCND) and entering the hot side (Evaporator, iEVP) of the MD unit
- MD distillate rate produced (D)
- Power produced by the RESs (Wnet). This value is partly accounted for in the batteries terminals (see discussion section).

A previous paper dealing with the experimental PVT validation has been taken to select the comparative statistic parameters [51]. In the comparison of the simulated and experimental measurements, the correlation coefficient (r) and root mean square percent deviation (e, %) have been evaluated by using the next equations:

$$r = \frac{N\sqrt{X_i Y_i} - (\sum X_i)(\sum Y_i)}{\sqrt{N\sum X_i^2 - (\sum X_i)^2}\sqrt{N\sum Y_i^2 - (\sum Y_i)^2}} \quad (1)$$

$$e = \sqrt{\frac{\sum (e_i)^2}{N}} = \sqrt{\frac{\sum\left(\left[\frac{X_i - Y_i}{X_i}\right]x100\right)^2}{N}} \quad (2)$$

where N is the number of values of the test, X_i are the theoretical (simulated) values and Y_i the experimental ones. Apart from those parameters, averaged value (MN), standard deviation (SD) as well as averaged relative error of calculated (c) and measured (r) variables (ARE, %) were also included in the analysis. In case of accumulative variables (D, E_{PU}) related to the plant demands, their amounts were also compared (see the two last blocks of three rows in Table 4).

3. Results and discussion

The results of the three analysed days are reported in Table 4. As it can be seen from those results, as a rule a good agreement has been found after an in-depth adjustment of the TRNSYS model according to the experimental values. Adjustable parameters included in types were moved in the reasonable margins in order to find out this accuracy. The root mean square percent deviation *e* and averaged relative error *ARE* are less than 10%, being the correlation coefficient *r* in the range 0.9-0.98 in most of the compared values, except from the test made on 06/03/18. In any case, a more detailed analysis of the largest deviations observed is presented next, and specific analysis of that test is presented hereafter.

Table 4. Comparison between experimental and simulated values.

Data	Test	r	e %	MN_r	SD_r	MN_c	SD_c	ARE %
T_{iPVT}	10/08	0.9352	8.42	60.74	6.08	63.16	9.71	7.85
(°C)	08/09	0.9008	10.82	64.03	4.44	68.34	4.60	11.26
	02/10	0.9108	16.29	67.76	0.74	76.21	3.29	16.23
	07/03	0.9286	8.50	54.35	5.57	57.97	11.14	7.91
	06/03	0.9326	27.23	31.40	7.14	36.52	10.52	25.146
T_{oPVT}	10/08	0.9054	11.13	63.39	5.80	68.67	9.44	9.17
(°C)	08/09	0.8766	7.90	66.02	5.21	77.48	5.78	10.08
	02/10	0.9737	13.15	70.49	1.04	80.07	7.04	13.41
	07/03	0.9617	10.61	56.91	10.79	62.09	16.5	16.91
	06/03	0.7014	69.16	38.63	6.9	52.25	27.95	53.08
T_{oETC}	10/08	0.8455	13.56	65.33	4.95	71.14	10.07	10.21
(°C)	08/09	0.9546	8.79	67.90	3.90	74.13	6.13	11.51
	02/10	0.9565	16.47	71.28	1.07	82.30	5.15	18.61
	07/03	0.8629	13.53	61.48	5.57	69.46	20.52	21.75
	06/03	0.5663	93.66	54.41	4.10	76.20	52.98	68.19
T_{uHWT}	10/08	0.9708	5.04	58.53	7.07	58.66	9.12	4.13
(°C)	08/09	0.9815	4.98	60.38	4.11	62.97	3.76	4.43
	02/10	0.9334	9.94	63.28	0.67	69.34	1.44	9.59
	07/03	0.9599	5.27	56.70	7.4	57.30	6.61	3.72
	06/03	0.7681	41.00	55.60	1.49	37.26	3.87	32.42
T_{dHWT}	10/08	0.9711	24.73	59.90	4.97	48.45	12.05	20.22
(°C)	08/09	0.9936	7.28	62.60	4.15	58.07	3.62	8.62
	02/10	0.9914	6.20	67.04	0.64	63.16	1.10	5.84
	07/03	0.8093	19.28	57.10	4.8	48.56	8.78	15.39
	06/03	0.8712	32.89	44.26	9.35	55.57	2.17	32.77
T_{mHWT}	10/08	0.9882	18.85	59.22	5.91	50.86	11.20	15.20
(°C)	08/09	0.9314	5.96	61.49	4.12	58.73	3.29	5.13
	02/10	0.9549	2.12	65.16	0.61	64.61	0.94	1.84
	07/03	0.8748	14.73	56.68	4.95	50.57	7.95	11.23
	06/03	0.9825	21.52	52.63	2.27	41.16	3.14	21.86
T_{oCND}	10/08	0.9765	12.11	42.01	18.01	41.76	19.58	6.10
(°C)	08/09	0.9864	1.22	58.36	3.92	58.69	3.85	0.78
	02/10	0.9409	4.87	61.35	0.55	61.99	1.15	2.20
	07/03	0.9847	15.71	42.26	15.82	42.59	17.42	6.53
	06/03	0.9934	11.74	19.25	0.79	16.98	0.71	11.73
T_{iEVP}	10/08	0.9827	10.01	44.39	20.62	43.90	21.7	4.54

(°C)	08/09	0.9845	1.17	63.14	4.22	63.01	4.13	0.88
	02/10	0.9866	2.55	67.04	0.64	67.74	1.32	2.26
	07/03	0.9935	11.12	46.38	19.4	46.29	19.89	3.27
	06/03	0.9975	5.76	18.02	0.72	16.98	0.71	5.75
D	10/08	0.9480	15.40	5.47	0.56	5.99	0.37	10.95
(L/h)	08/09	0.9282	9.48	5.81	1.04	5.82	0.91	3.26
	02/10	0.9415	7.56	8.79	0.22	8.48	0.46	5.95
	07/03	0.9142	23.89	8.47	1.29	9.97	1.30	18.72
	06/03	--	--	--	--	--	--	--
W_{net}	10/08	0.9631	69.71	421.1	260.9	440.1	272.0	17.21
(W)	08/09	0.9883	10.94	436.0	163.7	432.9	173.9	6.49
	02/10	0.8339	49.83	557.4	122.7	560.9	144.6	20.78
	07/03	0.9790	15.71	458.2	207.9	485.3	222.5	23.70
	06/03	0.7792	473.7	283.63	232.2	309.9	237.5	108.8
D_{TOT}	10/08			19.24		21.08		8.75
(L/test)	08/09			51.36		51.40		0.08
	02/10			33.69		32.49		-3.70
	07/03			50.10		58.98		15.05
	06/03			--		--		--
$E_{PU,TOT}$	10/08			3361.9		3513.2		4.30
(Wh/test)	08/09			3924.2		3896.5		0.71
	02/10			2229.6		2243.7		0.63
	07/03			3470.4		3661.2		-5.50
	06/03			1512.7		1653.2		-9.28

Regarding the desalting units, it is noticed that the RO is almost insensitive to plant operation whenever enough SOC is found in batteries. Thus, it has been modelled in TRNSYS17 by a constant internal power demand. On the contrary, MD is quite responsive to plant operation or environmental conditions. For instance, the rather high readings found for standard deviations in day 10/08/2017 are related to the unsteady profile of solar input (see Figure 3). Besides, the typical MD behaviour can be explained with Figure 5 including the compared temperature profiles and distillate rates of the MD unit for the second day analysed (08/09/2017). First, distillate start up depends on the time lasted from previous tests. This means that the MD unit requires a rather long period to warm the canals (about 20-30 minutes) in the worst case, which is not controlled by the model. Second, the ANN is less sensitive to small random variations that continuously were observed in the MD operation. This is mainly due to the MD feedwater pump operation, which consumes DC converted by the AC supply from the inverter. This can be confirmed in the flowrate reduction in the test at noon, being the MD response higher than the one predicted by the ANN characterizing the MD model.

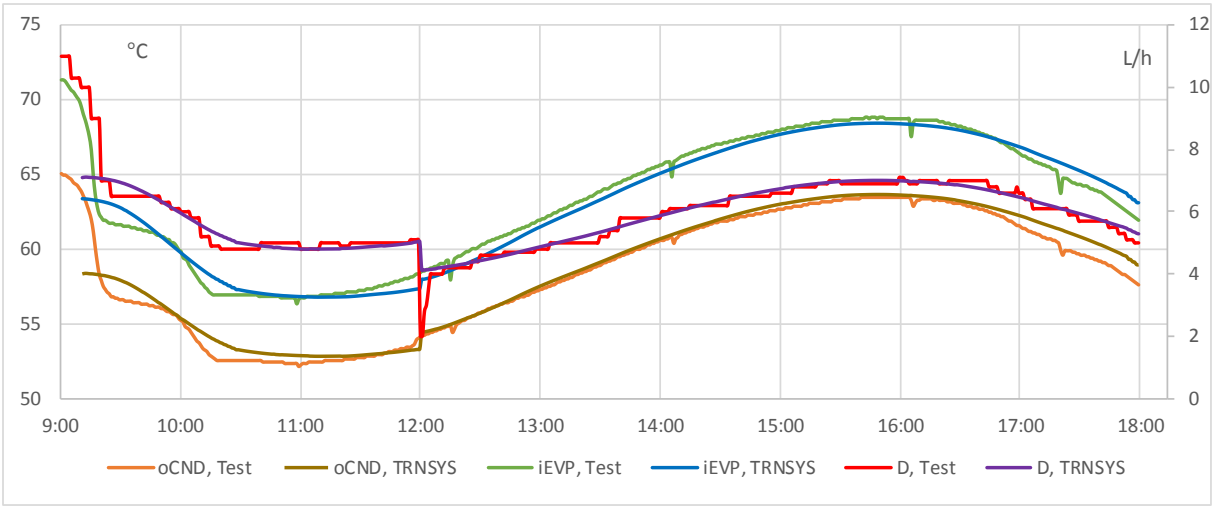

Figure 5. MD temperatures (left) and production (right, experimental and simulated, 08/09/2017)

If the targeted approach is on the solar loop, some deviations have been found in some subsystems and especially at the start of the tests. For instance, solar loop temperatures of the leaving PVT and ETC were unsteady at the sun rising and the sunset (see Figure 6 for day 10/08/2017) in which solar pump is alternatively switched on and off every few seconds. Experimentally this could be solved by using a variable feed pump. High noise level found in simulated values is due to the large time step for simulation, which is equal to the one used for instrumentation but obviously should be reduced in TRNSYS. Temperatures in the HWT also provided some discrepancies in some days but not in others at the test starting period in the simulation of a stratified HWT (see Figure 6 corresponding to the third test, 02/10/2017). First, it should be considered that the two PT-100 sensors used are physically more closely than the nodes in the stratified tank model. Nevertheless, in this Figure it can be clearly seen that once the feed pump to the HX-MD is operating from 13:10 approximately, a constant and rather low temperature gap of about 4°C between the upper and lower temperatures is found. This is provoked by the constant recirculation of hot water leaving and then returning with some degrees below to the tank, after being heated the MD condenser canal. Obviously the HWT tank model does not consider this effect and therefore higher gaps were usually found in simulations.

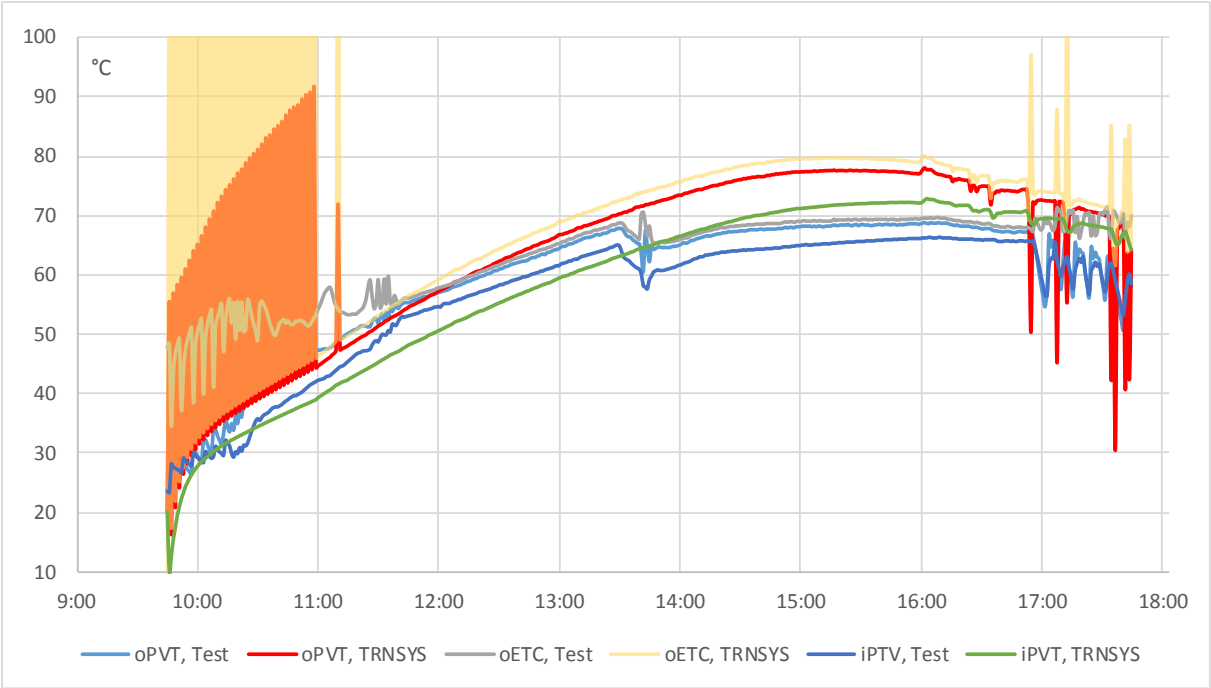

Figure 6. Validation of solar loop temperatures (10/08/2017). Note that red colour has been degraded to see leaving ETC temperature

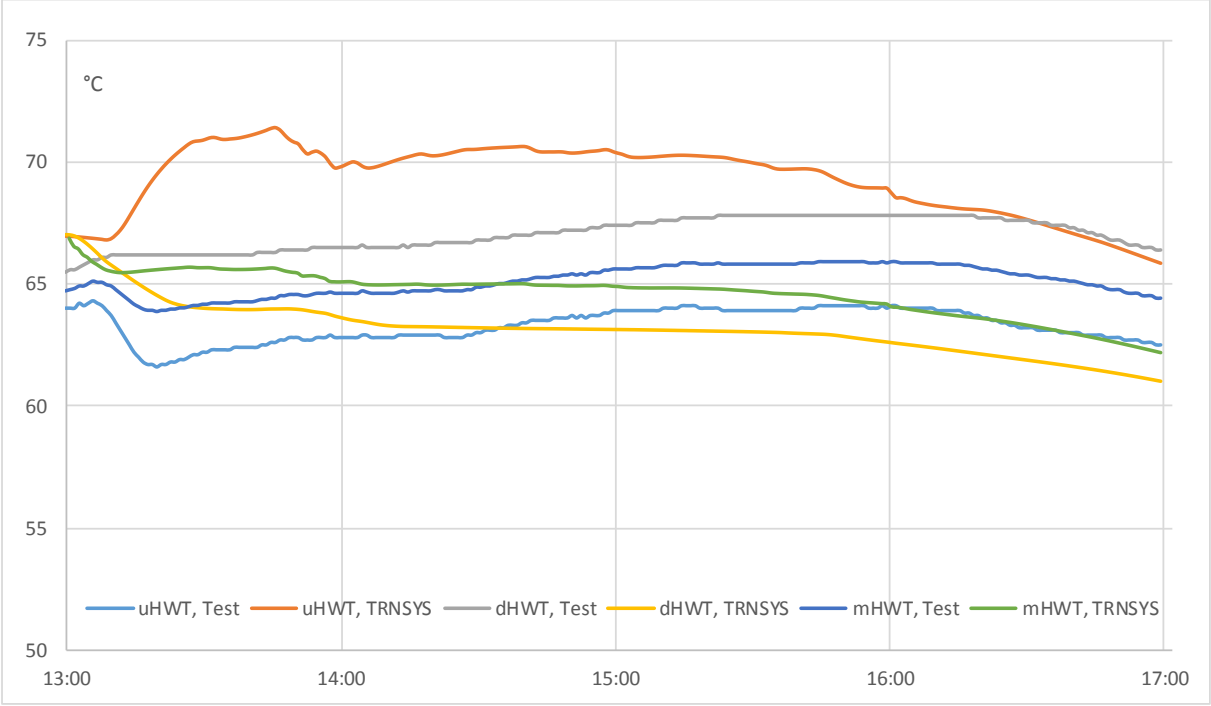

Figure 7. Hot Water Tank temperatures validation (02/10/2017).

Finally, net power produced in the plant is rather difficult to compare with (see Figure 8 and the analysis of 08/09/2017). It is usual that standard deviation SD must be high since net power increases a lot during the test up to noon and then decreases symmetrically if weather variations are not found. However, relative error ARE should be lower than 10% as in the other measures. Several reasons are responsible for this amount. First, it is important to remember that power in

test values is roughly estimated. Power value entering or leaving to the batteries terminals is measured, then auxiliary pumps and cooler consumptions were added. Those consumptions were taken from previous individual tests at diverse plant loads but they could be changed along the plant life. Secondly, one unexpected result from lab test was the scarce contribution of the WT to the power supply, mainly due to its difficult positioning and non-manipulable charge controller, being the production lower than the expected by the WT power curve included in the model. Secondly, potentiometer to simulate the home internal demand has a variable conversion efficiency since power given by the digital readout and the equivalent in the batteries terminals may lead to a diversion of up to 15%. Finally, data recording to the memory card linked to the automata takes about 35 seconds to write the whole set of measures every time step. Then, some peaks could be explained by the fact that one pump or the cooler could be activated at the time that was recorded, but not at the time that power in the batteries terminals was taken (maybe 25-30 seconds before) for that step.

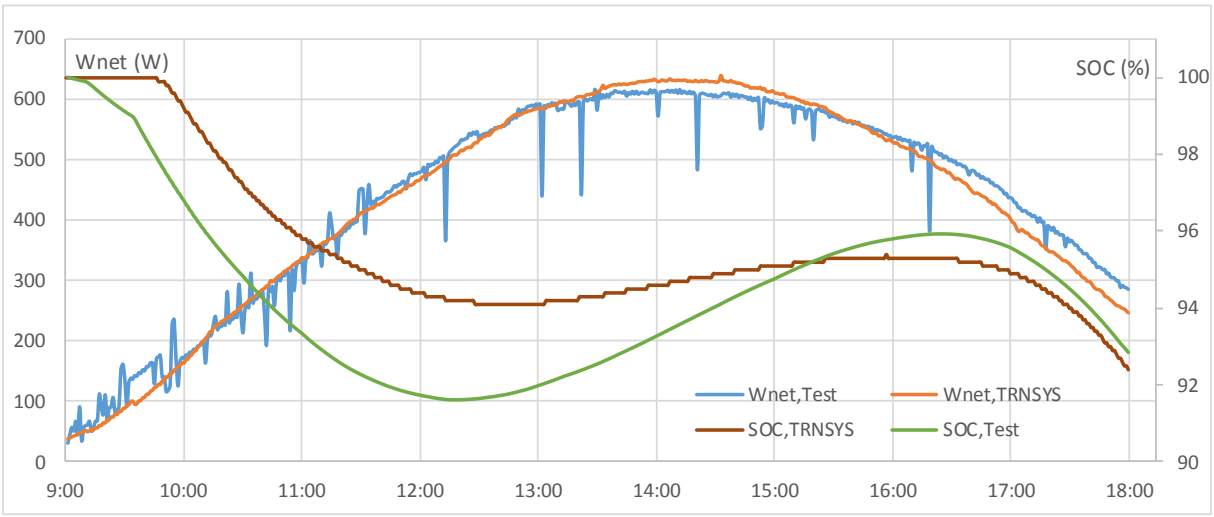

Figure 8. Validation of the net power produced (left) and battery level (right) in the plant (08/09/2017).

Validation of the SOC values shows that the battery use and hot weather have provoked higher discharge and charge rates of the batteries in real conditions but not for all the validated tests. Therefore, some adjustments in the TRNSYS types modelling the batteries should be made according to the life time and weather inputs, taking into account that the existing ones have not yet reached the maximum depth of discharge suggested by the manufacturer.

Table 4 also shows some high values of the statistical parameters; they correspond to the daytime test on 06/03/2018 corresponding to drastic but continuous changes in solar irradiation and wind profile. Combination of stochastic external parameters and delay already mentioned in the card recording seem to be the main reasons for the discrepancies between measured and simulated values. Next figure shows the main external parameters as well as the main productions of the pilot plan that daytime test.

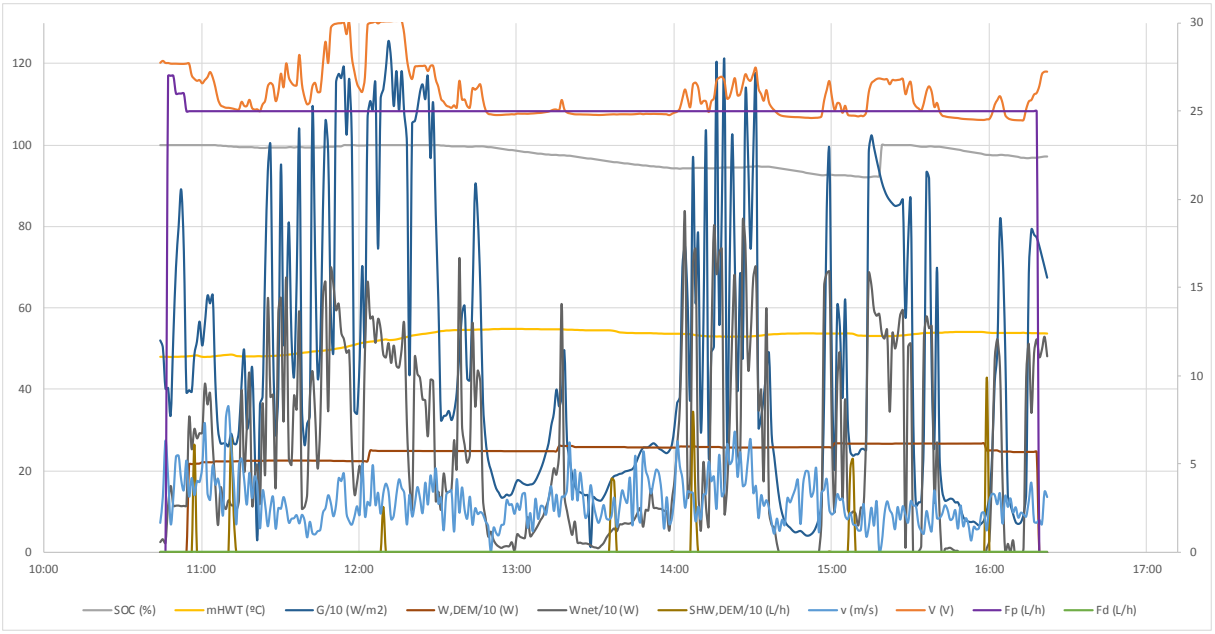

Figure 9. External conditions, productions and energy levels in the daytime test 06/03/2018. From wind velocity (blue line), right axe should be taken.

4. Conclusions

A new simulation model of a small hybrid RES unit that provides power, SHW and desalted water by hybrid desalination to serve an isolated family home has been developed in TRNSYS17 and then validated by experimental data selected from the test campaign of the pilot unit. Selected days combine some typical weather conditions and operating rules applied on the tests. Measured data from experimental analysis showed that the model could give the adequate response of the daytime thermal and electric demands at different climatic conditions. Slight differences between measured and simulated data were found in some points. Those differences are enlarged in very unstable conditions of the available solar and wind resources. Main reason for the inaccuracy of the model with respect to the pilot unit is related to some limitations to include detailed aspects of the pilot unit operation. Uncontrolled transitory effects like the SWT stratification or any manual operation in the pilot plant are additional error sources that could not be fully considered in the model. For instance, hourly SHW demand could be covered in only 1 minute but this demand is steadily served in TRNSYS. Cooling system of the MD unit was not implemented in TRNSYS, as well as the SWT. Some of the limitations related to the model could be adjusted in TRNSYS, for instance the adequacy of the WT curves to a more real physical production based on the tests, or the HX efficiencies and loss coefficients of the PVT, ETC, and so on. A different time step than the used in tests is also required to reduce the amount of noise in the sunrise and sunset periods, while in the other side could be solved by using a variable flow pump. An accurate prediction of the MD distillate in TRNSYS is also required since the amount of heat required provokes a cascade effect through the HWT and then even in the solar loop.

Nonetheless, deviations coming from the pilot plant are more complicated to solve. A better accuracy of the instrumentation or a higher frequency in the monitoring could be obtained with a new system. Calibration has to be very intensive to properly measure the whole set of temperatures and therefore the heat supplied to each plant subsystem. Nonetheless, and considering the present uncertainty associated to the measured parameters analysed, found

differences could be reasonably assumed, taking into account that they come from both sides (experimental and modelling).

Major advantage of this plant is the reliability of the sustainable water provision by means of two complementary desalination techniques supplied by RES and consuming power and heat respectively. As stated in [41], the scale-up of this hybrid trigeneration scheme to any other demand profiles could be carried out by the help of this validated model. As the pilot unit is based on modular devices, new plants could be built by only increasing the number of PVT, ETC, WT or RO/MD units and the capacities of the batteries and the HWT. Therefore, such new plants can be easily adapted to higher demands of power, SHW and water with lower production costs due to economies of scale.

Acknolegments

This work has been supported by the Spanish Ministry of Economics and Competitiveness (R+D Project ENE2014-59947-R) and the Government of Aragón (Research Group T28-17R). It was previously presented at the 14th Conference on Sustainable Development of Energy, Water and Environmental Systems (SDEWES), held in Dubrovnik from 1st to 6th October 2019 with the title "Validation of the Experimental Tests of a Domestic Trigeneration Scheme with Hybrid RESs and Desalting Techniques"

NOMENCLATURE

AC	Alternating Current / Air Cooled
ANN	Artificial Neural Network
ARE	Averaged relative error (%)
C	Conductivity (μS/cm)
CR	Coverage Rate (%)
D	Distillate (from MD, L/h)
DC	Direct Current
e	Root mean square percent deviation (%)
E	Electricity (Wh)
ER	Electric Resistance (variable)
ETC	Evacuated Tube Collector
F	Flow rate (L/h)
Fd	Distillate flowrate (from MD)
Fp	Permeate flowrate (from RO)
FPC	Flat Plate Collector
FW	Fresh Water (desalted, L/h)
G	Irradiation (total, W/m^2)
HX	Heat Exchanger
HWT	Hot Water Tank
I	Current (A)
m	Averaged data
MD	Membrane Distillation
MPPT	Maximum Power Point Tracker
P	Pump
PG	Permeate Gap (MD type)
PV	Photovoltaics
PVT	Photovoltaic-Thermal collector
RES	Renewable Energy Source
RO	Reverse Osmosis

SD	Standard deviation
SEC	Specific Energy Consumption (kWh/m^3)
SHW	Sanitary Hot Water
SOC	Stage of Charge (%)
SW	Seawater
SWT	Sea Water Tank
T	Temperature (°C)
TF	Thermal fraction (%)
U	Uncertainty (%)
v	Wind velocity (m/s)
V	Voltage (V)
W	Power (W)
WEN	Water and Energy Nexus
WF	Power fraction (%)
WT	Wind Turbine
X	Theoretical (simulated) data
Y	Measured data

Subscripts

c	Calculated (simulated)
CND	Condenser (cold MD canal)
d	Down (lower)
EVP	Evaporator (hot MD canal)
H	Home (internal power demand)
i	Inlet
m	Medium
net	Net (power)
o	Outlet
p	Peak
PU	Pilot unit
PVT	Photovoltaics
r	Real (measured)
SL	Solar Loop
TOT	Total
u	Upper
WT	Wind turbine

REFERENCES

[1] C.M. Papapostolou, E.M. Kondili, D.P. Zafirakis, G.T. Tzanes, Sustainable water supply systems for the islands: The integration with the energy problem, Renew. Energy 146 (2020) 2577-2588. https://doi.org/10.1016/j.renene.2019.07.130

[2] Editorial. Sustainable development using renewable energy technology. Renew. Energy 146 (2020) 2430-2437. https://doi.org/10.1016/j.renene.2019.08.094

[3] I. Kougias, S. Szabo, A. Nikitas, N. Theodossiou, Sustainable energy modelling of non-interconnected Mediterranean, Renew. Energy 133 (2019) 930-940. https://doi.org/10.1016/j.renene.2018.10.090

[4] V. Bakic, M. Pezo, Z. Stevanovic, M. Zivkovic, B. Grubor, Dynamical simulation of PV/wind hybrid energy conversion system. Energy 45 (2012), 324-328. doi:10.1016/j.energy.2011.11.063.

[5] M. Bertsiou, E. Feloni, D. Karpouzos, E. Baltas, Water management and electricity output of a Hybrid Renewable Energy System (HRES) in Fournoi Island in Aegean Sea, Renew. Energy 118 (2018) 790-798. https://doi.org/10.1016/j.renene.2017.11.078
[6] T. Ma, H. Yang, L. Lu, J. Peng, Technical feasibility study on a standalone hybrid solar-wind system with pumped hydro storage for a remote island in Hong Kong, Renew. Energy 69 (2014) 7-15. http://dx.doi.org/10.1016/j.renene.2014.03.028
[7] X. Xu, W. Hu, D. Cao, Q. Huang, C. Chen, Z. Chen. Optimized sizing of a standalone PV-wind-hydropower station with pumped-storage installation hybrid energy system. Renew. Energy 147 (2020) 1418-1431. https://doi.org/10.1016/j.renene.2019.09.099
[8] A. Buonomano, F. Calise, A. Palombo, M. Vicidomini, Adsorption chiller operation by recovering low-temperature heat from building integrated photovoltaic thermal collectors: Modelling and simulation, Energy Convers. Manag, 149 (2017), 1019-1036. http://dx.doi.org/10.1016/j.enconman.2017.05.005
[9] A. Kasaeian, F. Rajaee, W.M. Yan, Osmotic desalination by solar energy: A critical review, Renew. Energy 134 (2019) 1473-1490. https://doi.org/10.1016/j.renene.2018.09.038
[10] I.B. Askari, M. Ameri, Solar Rankine Cycle (SRC) powered by Linear Fresnel solar field and integrated with Multi Effect Desalination (MED) system, Renew. Energy 117 (2018) 52-70. https://doi.org/10.1016/j.renene.2017.10.033
[11] J.S. Solís-Chaves, C.M. Rocha-Osorio, A.L.L. Murari, V. M. Lira, A. J. Sguarezi, Extracting potable water from humid air plus electric wind generation: A possible application for a Brazilian prototype, Renew. Energy 121 (2018) 102-115. https://doi.org/10.1016/j.renene.2017.12.039
[12] Y. Wu, T. Ming, R. de Richter, R. Hoffer, H.J. Niemann Large-scale freshwater generation from the humid air using the modified solar chimney, Renew. Energy 146 (2020) 1325-1336. https://doi.org/10.1016/j.renene.2019.07.061
[13] F. E. Ahmed, R. Hashaikeh, N. Hilal Solar powered desalination – Technology, energy and future outlook, Desalination 453 (2019) 54–76. https://doi.org/10.1016/j.desal.2018.12.002
[14] V.G. Gude, Energy storage for desalination processes powered by renewable energy and waste heat sources. Appl. Energy 137 (2015) 877-898. http://dx.doi.org/10.1016/j.apenergy.2014.06.061
[15] K. Srithar, T. Rajaseenivasan, N. Karthik, M. Periyannan, M. Gowtham, Stand alone triple basin solar desalination system with cover cooling and parabolic dish concentrator, Renew. Energy 90 (2016) 157-165. http://dx.doi.org/10.1016/j.renene.2015.12.063
[16] H. Cherif, J. Belhadj, Large-scale time evaluation for energy estimation of stand-alone hybrid photovoltaic wind system feeding a reverse osmosis desalination unit. Energy 36 (10) (2011), 6058-6067. doi:10.1016/j.energy.2011.08.010
[17] H. Mokhtari, M. Sepahv, A. Fasihfar, Thermoeconomic and exergy analysis in using hybrid systems (GT+MED+RO) for desalination of brackish water in Persian Gulf. Desalination 399 (2016) 1-15. http://dx.doi.org/10.1016/j.desal.2016.07.044
[18] S. Sadri, R.H. Khoshkhoo, M. Ameri, Optimum exergoeconomic modeling of novel hybrid desalination, Energy 149 (2018) 74-83 https://doi.org/10.1016/j.energy.2018.02.006
[19] G. Filippini, M.A. Al-Obaidib, F. Manentia, I.M. Mujtabab. Design and economic evaluation of solar-powered hybrid multi effect and reverse osmosis system for seawater desalination, Desalination 465 (2019) 114–125. https://doi.org/10.1016/j.desal.2019.04.016

[20] A.E. Kabeel, E.M.S. El-Said, Experimental study on a modified solar power driven hybrid desalination system, Desalination 443 (2018) 1–10. https://doi.org/10.1016/j.desal.2018.05.017
[21] M.A.M. Khan, S. Rehman, F. A. Al-Sulaiman A hybrid renewable energy system as a potential energy source for water desalination using reverse osmosis: A review Renewable and Sustainable Energy Reviews 97 (2018) 456–477 https://doi.org/10.1016/j.rser.2018.08.049
[22] W. Peng, A. Maleki, M.A. Rosen, P. Azarikhah Optimization of a hybrid system for solar-wind-based water desalination by reverse osmosis: Comparison of approaches Desalination 442 (2018) 16–31 https://doi.org/10.1016/j.desal.2018.03.021
[23] F. Calise, M. Dentice d'Accadia, M. Vicidomini, Optimization and dynamic analysis of a novel polygeneration system producing heat, cool and fresh water, Renew. Energy 143 (2019) 1331-1347. https://doi.org/10.1016/j.renene.2019.05.051
[24] F. Calise, M. Dentice d'Accadia, A: Macaluso, A. Piacentino, L. Vanoli, Exergetic and exergoeconomic analysis of a novel hybrid solar–geothermal polygeneration system producing energy and water, Energy Convers. Manag. 115 (2016) 200–220. http://dx.doi.org/10.1016/j.enconman.2016.02.029
[25] F. Calise, A. Cipollina, M. Dentice d'Accadia, A. Piacentino, A novel renewable polygeneration system for a small Mediterranean volcanic island for the combined production of energy and water: Dynamic simulation and economic assessment, Appl. Energy 135 (2014) 675-693. http://dx.doi.org/10.1016/j.apenergy.2014.03.064
[26] F. Calise, M. Dentice d'Accadia, A. Piacentino, A novel solar trigeneration system integrating PVT (photovoltaic/thermal collectors) and SW (seawater) desalination: Dynamic simulation and economic assessment, Energy 67 (2014) 129-148. http://dx.doi.org/10.1016/j.energy.2013.12.060
[27] F. Calise, M. Dentice d'Accadia, A. Piacentino, M. Vicidomini, Thermoeconomic optimization of a renewable polygeneration system serving a small isolated community, Energies 8 (2015), 995-1024. doi:10.3390/en8020995
[28] F. Calise, A. Macaluso, A. Piacentino, L. Vanoli, A novel hybrid polygeneration system supplying energy and desalinated water by renewable sources in Pantelleria Island, Energy 137 (2017), 1086-1106. http://dx.doi.org/10.1016/j.energy.2017.03.165
[29] F. Calise, M. Dentice d'Accadia, L. Vanoli, M. Vicidomini, Transient analysis of solar polygeneration systems including seawater desalination: A comparison between linear Fresnel and evacuated solar collectors, Energy 172 (2019) 647-660. https://doi.org/10.1016/j.energy.2019.02.001
[30] D. Coppitters, F. Contino, A. El-Baz, P. Breuhaus, W. De Paepe, Techno-economic feasibility study of a solar-powered distributed cogeneration system producing power and distillate water: Sensitivity and exergy analysis, Renew. Energy (In press), https://doi.org/10.1016/j.renene.2019.10.105
[31] B. Ghorbani, K.B. Mahyari, M. Mehrpooya, Introducing a hybrid renewable energy system for production of power and fresh water using parabolic trough solar collectors and LNG cold energy recovery. Renew. Energy (In press), https://doi.org/10.1016/j.renene.2019.10.063
[32] C. Mata-Torres, R. Escobar, J.M. Cardemil, Y. Simsek, J.A. Matute, Solar polygeneration for electricity production and desalination: Case studies in Venezuela and northern Chile, Renew. Energy 101 (2017), 387-398. http://dx.doi.org/10.1016/j.renene.2016.08.068
[33] G. Mohan, N.T.U. Kumar, M.K. Pokhrel, A. Martin, A novel solar thermal polygeneration system for sustainable production of cooling, clean water and domestic

hot water in United Arab Emirates: dynamic simulation and economic evaluation. Appl. Energy 167 (2016) 173-188. http://dx.doi.org/10.1016/j.apenergy.2015.10.116

[34] M. Yari, L. Ariyanfar, E.A. Aghdam, Analysis and performance assessment of a novel ORC based multigeneration system for power, distilled water and heat, Renew. Energy 119 (2018) 262-281. https://doi.org/10.1016/j.renene.2017.12.021

[35] P. Behnama, A. Arefi, M. B. Shafii, Exergetic and thermoeconomic analysis of a trigeneration system producing electricity, hot water, and fresh water driven by low-temperature geothermal sources, Energy Convers. Manag. 157 (2018) 266–276. https://doi.org/10.1016/j.enconman.2017.12.014

[36] R. Leiva-Illanes, R. Escobar, J.M. Cardemil, D.C. Alarcón-Padilla, Thermoeconomic assessment of a solar polygeneration plant for electricity, water, cooling and heating in high direct normal irradiation conditions, Energy Convers. Manag. 151 (2017) 538–552. http://dx.doi.org/10.1016/j.enconman.2017.09.002

[37] R. Leiva-Illanes, R. Escobar, J.M. Cardemil, D.C. Alarcón-Padilla, J. Uche, A. Martínez, Exergy cost assessment of CSP driven multi-generation schemes: Integrating seawater desalination, refrigeration, and process heat plants, Energy Convers. Manag. 179 (2019) 249–269. https://doi.org/10.1016/j.enconman.2018.10.050

[38] G. Zhang, B. Wua, A. Malekib, W. Zhang, Simulated annealing-chaotic search algorithm based optimization of reverse osmosis hybrid desalination system driven by wind and solar energies, Sol. Energy 173 (2018) 964–975, https://doi.org/10.1016/j.solener.2018.07.094

[39] E. Baniasadi, Concurrent hydrogen and water production from brine water based on solar spectrum splitting: Process design and thermoeconomic analysis, Renew. Energy 102 (2017) 50-64. http://dx.doi.org/10.1016/j.renene.2016.10.042

[40] U. Sahoo, R. Kumar, R., P.C. Pant, R. Chaudhury, Scope and sustainability of hybrid solar-biomass power plant with cooling, desalination in polygeneration process in India. Renew. Sustain. Energy Rev., 51 (2015), 304-316. http://dx.doi.org/10.1016/j.rser.2015.06.004

[41] J. Uche, L. Acevedo, F. Círez, S. Usón, A. Martínez-Gracia, A.A. Bayod, Analysis of a domestic trigeneration scheme with hybrid renewable energy sources and desalting techniques, J. Clean. Prod. 212 (2019), 1409-1422. https://doi.org/10.1016/j.jclepro.2018.12.006

[42] M.E. Demir, I. Dincer., Development of an integrated hybrid solar thermal, power system with thermoelectric generator for desalination and power production, Desalination, 404 (2017), 59-71. http://dx.doi.org/10.1016/j.desal.2016.10.016

[43] M. Esrafilian, R. Ahmadi, Energy, Energy, environmental and economic assessment of a polygeneration system of local desalination and CCHP, Desalination 454 (2019), 20–37. https://doi.org/10.1016/j.desal.2018.12.004

[44] D. Maraver, J. Uche, J. Royo, Assessment of high temperature organic Rankine cycle engine for polygeneration with MED desalination: a preliminary approach. Energy Convers. Manag. 53(1), (2011), 108-117. doi:10.1016/j.enconman.2011.08.013

[45] M. Luqman, T. Al-Ansari Thermodynamic analysis of a Energy-Water-Food (Ewf) nexus driven polygeneration system applied to coastal communities Energy Conversion and Management 205 (2020) 112432 https://doi.org/10.1016/j.enconman.2019.112432

[46] B. Ghorbani, K.B. Mahyari, M. Mehrpooya, M.H. Hamedi Introducing a hybrid renewable energy system for production of power and fresh water using parabolic trough solar collectors and LNG cold energy recovery Renewable Energy 148 (2020) 1227e1243 https://doi.org/10.1016/j.renene.2019.10.063

[47] A. Juárez, I. Domínguez, T. Herrera, Using TRNSYS® simulation to optimize the design of a solar water distillation system, Ene. Procedia 57 (2014), 2441-2450. doi: 10.1016/j.egypro.2014.10.253

[48] R.G. Raluy, R. Schwantes, V. Subiela, B. Peñate, G. Melián, J. Betancort, Operational experience of a solar membrane distillation demonstration plant in Pozo Izquierdo-Gran Canaria Island (Spain), Desalination 290 (2012), 1-13. doi:10.1016/j.desal.2012.01.003

[49] A. Chafidz, E.D. Kerme, I. Wazeer, Y. Khalid, A. Ajbar, S.M. Al-Zahrani, Design and fabrication of a portable and hybrid solar-powered membrane distillation system, J. Clean. Prod. 133 (2016), 631-647. http://dx.doi.org/10.1016/j.jclepro.2016.05.127

[50] A.M. Manokar, D.P. Winston, A.E. Kabeel, R. Sathyamurthy, Sustainable fresh water and power production by integrating PV panel in inclined solar still, J. Clean. Prod., 172 (2018) 2711-2719. https://doi.org/10.1016/j.jclepro.2017.11.140

[51] G. Mohan, N.T.U. Kumar, M.K. Pokhrel, A. Martin, A., Experimental investigation of a novel solar thermal polygeneration plant in United Arab Emirates. Renew. Energy 91 (2016) 361-373. http://dx.doi.org/10.1016/j.renene.2016.01.072

[52] A.M. Elzahaby, A.E. Kabeel, M.M. Bassuoni, A, Refat, A. Elbar, Direct contact membrane water distillation assisted with solar energy. Energy Convers. Manag, 110 (2016), 397-406. http://dx.doi.org/10.1016/j.enconman.2015.12.046

[53] H. Chang, S.G. Lyu, C.M. Tsai, Y.H. Chen, T.W. Cheng, Y.H. Chou, Experimental and simulation study of a solar thermal driven membrane distillation desalination process, Desalination 286 (2012), 400-411. doi:10.1016/j.desal.2011.11.057

[54] W.G. Shim, K. He, S. Gray, I. S. Monn, Solar energy assisted direct contact membrane distillation (DCMD) process for seawater desalination. Separ. Purif. Technol., 143 (2015), 94-104. http://dx.doi.org/10.1016/j.seppur.2015.01.028

[55] T. Srinivas, B.V. Reddy, Hybrid solar-biomass power plant without energy storage. Case Studies in Thermal Engineering 2 (2014), 75-81. http://dx.doi.org/10.1016/j.csite.2013.12.004

[56] N. Aste, F. Leonforte, C. Del Pero, Design, modeling and performance monitoring of a photovoltaic–thermal (PVT) water collector, Sol. Energy 112 (2015) 85–99. http://dx.doi.org/10.1016/j.solener.2014.11.025

[57] R. Chaker, H. Dhaouadi, H. Mhiri, P. Bournot, A TRNSYS Dynamic Simulation Model for Photovoltaic System Powering a Reverse Osmosis Desalination Unit with Solar Energy, Int. Journal of Chem. Reac. Eng., 8 A28 (2010).

[58] A. Buonomano, F. Calise, M. Vicidomini, Design, simulation and experimental investigation of a solar system based on PV panels and PVT collectors. Energies 9 (2016) 497-504. doi:10.3390/en9070497

[59] P. Haurant, C. Ménézo, L. Gaillard, P. Dupeyrat, A numerical model of a solar domestic hot water system integrating hybrid photovoltaic/thermal collectors, Ene. Procedia 78 (2015) 1991–1997. doi: 10.1016/j.egypro.2015.11.391

[60] M. Sardarabadi, A. Naghdbishi, M.P. Fard, H. Sardarabadi, S.Z. Heris, Computer Modelling and Experimental Validation of a Photovoltaic Thermal (PV/T) Water Based Collector System, 2012 2nd International Conference on Power and Energy Systems (ICPES 2012), *IPCSIT*, Vol. 56, 2012, IACSIT Press, Singapore.

[61] A. Del Amo, A. Martínez, A.A. Bayod, J. Antonanza, An innovative urban energy system constituted by a photovoltaic/thermal hybrid solar installation: design, simulation and monitoring, Appl. Energy 186 (2017), 140-151. http://dx.doi.org/10.1016/j.apenergy.2016.07.011

[62] L. Cioccolanti, M. Villarini, R. Tascioni, E. Bocci, Performance assessment of a solar trigeneration system for residential applications by means of a modelling study, Ene. Procedia 126 (2017), 444-452. doi:10.1016/j.egypro.2017.08.211

[63] A. Moaleman, A. Kasaeian, M. Aramesh, O. Mahian, L. Sahota, G.N. Tiwari, Simulation of the performance of a solar concentrating photovoltaic-thermal collector, applied in a combined cooling heating and power generation system, Energy Convers. Manag, 160 (2018), 191-208. https://doi.org/10.1016/j.enconman.2017.12.057

[64] E. Akrami, A. Chitsaz, H. Nami, S.M.S. Mahmoudi, Energetic and exergoeconomic assessment of a multi-generation energy system based on indirect use of geothermal energy, Energy 124 (2017), 625-639. http://dx.doi.org/10.1016/j.energy.2017.02.006

[65] L. Acevedo, J. Uche, A. Del Almo, F. Círez, S. Usón, A. Martínez, I. Guedea, Dynamic simulation of a trigeneration scheme for domestic purposes based on hybrid techniques. Energies 9 (2016), 1013. doi:10.3390/en9121013

[66] A.A. Bayod, A. Martínez, L. Acevedo, J. Uche, S. Usón, Improved management of battery and fresh water production in grid connected PVT systems in dwellings. *10th BIWAES Biennial International Workshop Advances in Energy Studies*, Naples, Italy, 25-28 September 2017. Graz University of Technology, Austria.

[67] S. Usón, J. Uche, A. Martínez, A. Del Amo, L. Acevedo, A.A. Bayod, Exergy assessment and exergy cost analysis of a renewable-based and hybrid trigeneration scheme for domestic water and energy supply. Energy 168 (2019), 662-683. https://doi.org/10.1016/j.energy.2018.11.124

[68] L. Acevedo, J. Uche, A. Del Almo, Improving the distillate prediction of a membrane distillation unit in a trigeneration scheme by using Artificial Neural Networks, Water10 (2018), 310. doi:10.3390/w10030310

[69] F. González, T. Rueda, S. Les, Microcomponentes y factores explicativos del consumo doméstico de agua en la Comunidad de Madrid (in Spanish). Cuadernos de I+D+I. Canal de Isabel II, Madrid, Spain, 2008.

[70] Red Eléctrica Española, S. A. (REE), Atlas de la demanda eléctrica. Proyecto INDEL, Madrid (in Spanish), 1998.

[71] Boletín Oficial del Estado (BOE-A-2016-12487, in Spanish). Resolución de 28 de diciembre de 2016, de la Dirección General de Política Energética y Minas, por la que se aprueba para el año 2017 el perfil de consumo y el método de cálculo a efectos de liquidación de energía, aplicables para aquellos consumidores tipo 4 y tipo 5 que no dispongan de registro horario de consumo, según el Real Decreto 1110/2007, de 24 de agosto, por el que se aprueba el reglamento unificado de puntos de medida del sistema eléctrico.

Credit Author Statement

Authors' individual contributions:

J. Uche: Writing – original draft, review & editing. Conceptualization, validation.

A. Muzás: Data curation, software.

L.E. Acevedo: Investigation, validation.

S. Usón: Editing – original draft & review

A. Martínez: Editing – review. Visualization.

A.A. Bayod: Supervision